[AMN04] Dynamic modelling of fuel cell system for mobile application using Simulink environment

Ahmad Raoof Ramli , Arshad Ahmad , Norazana Ibrahim , Lee Hock Weng

Laboratory of Process Control, Department of Chemical Engineering, Faculty of Chemical and Natural Resources Engineering, Universiti Teknologi Malaysia, 81310 Skudai, Johor, Malaysia.

Introduction

Nowadays, the increment of the petrol price has been a major problem for the consumers and it will increase more than 4 cent per litter in period of 6 to 12 month. Thus, there are many new energy developments that friendly to the environment have been commercialized to overcome this phenomenon such as solar energy and fuel cells technology. Among these, fuel cell power systems for transportation applications have received increased attention in recent years because of the potential for high fuel efficiency and lower emissions. A fuel cell converts hydrogen and oxygen into water, directly generating electrical energy from chemical energy without being restricted by efficiency limits of the Carnot thermal cycle (Larminie *et al*., 2000).

Proton exchange membrane (PEM) fuel cells are preferred for mobile application, because their low operating temperatures (around $80^{O}C$) and have provided more work from a given quantity of fuel and less polluting than internal combustion and gas turbine engines. Although, the limitation of hydrogen produce may become a minor problem, a fuel processor may be required to generate a hydrogen-rich stream using natural gas such as methane and methanol. So, the complete fuel cell system consists of a fuel processor unit and a PEM fuel cell stack unit as shown in Figure 1 and the aim of this study was to develop the plant simulation as a read for plantwide control configuration.
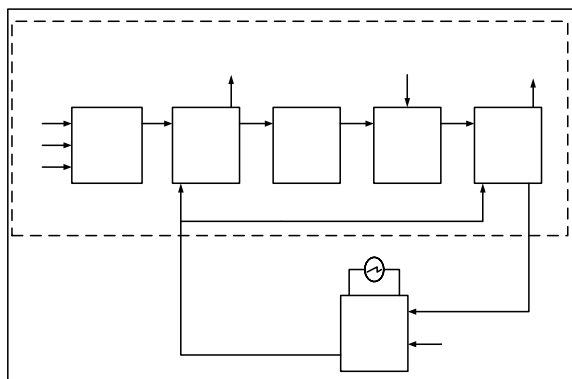

FIGURE 1   Flow diagram of PEM fuel cell plant

Material and Methods

The model development is divided into two main categories which are the development of the fuel processor and PEM fuel cell stack. The system generated a power of 5 kW and has been developed using Simulink environment (Matlab 6.5.1).

Fuel processor unit development

A fuel processor unit consists of an autothermal reactor (ATR), a water gas shift reactor (WGSR), a preferential oxidation reactor and two units of heat exchanger. The combinations of all these units produce a rich hydrogen stream and below 10 ppm CO concentration feed to PEM fuel cell stack.

Autothermal reactor mathematical model

A one-dimensional heterogeneous model is chosen in this work to simulate a tubular fixed-bed reactor. The mass and energy equations for the bulk and gas phase as well as the corresponding initial and boundary conditions are described below (De Smet *et al.,* 2001):

Gas phase

$$\varphi_m \frac{d}{dz}\left(\frac{C_i}{\rho_s} \right) + k_R a_V \left(C_i - C_{i,s}^{\,s} \right) = 0 \tag{1}$$

$$\varphi_m c_p \frac{dT_g}{dz} + h_f a_V \left(T_g - T_s \right) = 0 \tag{2}$$

Solid phase

$$\rho_f \frac{1}{r_p^2} \frac{D_{e,i}}{\varepsilon^2} \frac{d}{d\varepsilon}\left(\varepsilon^2 \frac{d}{d\varepsilon}\left(\frac{C_{i,s}}{\rho_f} \right) \right) + R_{w,i}\rho_s = 0 \tag{3}$$

$$h_f a_V \left(T_g - T_s \right) + \left(1 - \varepsilon_B \right)\Sigma\left(-\Delta_f H_i \right)\rho_s R_{w,i} = 0 \tag{4}$$

Gas-phase boundary conditions

$$z = 0 \quad\quad C_i = C_i^o \quad\quad T_g = T_g^o \tag{5}$$

Solid-phase boundary conditions

$$\varepsilon = 0 \quad\quad \frac{d}{d\varepsilon}\left(\frac{C_{i,s}}{\rho_f} \right) = 0 \tag{6}$$

$$\varepsilon = 1 \quad\quad \rho_f \frac{D_{e,i}}{r_p} \frac{d}{d\varepsilon}\left(\frac{C_{i,s}}{\rho_f} \right) = 0 \tag{7}$$

The simulation of the autothermal reaction is based on the following set of differential equations (Ann De Groote *et al.,* 1996).

Continuity Equations

$$\frac{dx_{CH_4}}{dz} = \frac{\rho_b \Omega}{F_{CH_4}^o} (\eta_1 r_1 - \eta_2 r_2 - \eta_3 r_3) \qquad (8)$$

$$\frac{dx_{O_2}}{dz} = \frac{\rho_b \Omega}{F_{O_2}^o} (2\eta_1 r_1) \qquad (9)$$

$$\frac{dx_{CO}}{dz} = \frac{\rho_b \Omega}{F_{CH_4}^o} (\eta_2 r_2) \qquad (10)$$

$$\frac{dx_{CO_2}}{dz} = \frac{\rho_b \Omega}{F_{CH_4}^o} (\eta_1 r_1 + \eta_3 r_3) \qquad (11)$$

Energy equation

$$\frac{dT}{dz} = \frac{\rho_b}{u_s \rho_g C_p} \Sigma \eta_i r_i (-\Delta H_i) \qquad (12)$$

The effectiveness factors, η are taken from an average value based upon a number of off-line pellet simulations for the various effectiveness factors (Ann De Groote *et al.,* 1996).

In the modelling of autothermal reforming of methane, it is necessary to combine all the rate equations for the total combustion, steam reforming for CO production and CO_2 production in the calculations. In this paper, the intrinsic reforming models (Xu *et al.,* 1989) are adopted as presented below. These authors derived the intrinsic rate equations for the steam reforming of methane on $Ni/MgAl_2O_3$ catalyst.

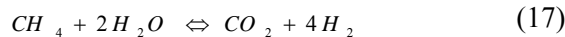Total oxidation

$$CH_4 + 2O_2 \Rightarrow CO_2 + 2H_2O \qquad (13)$$
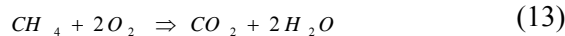
$$r_1 = \frac{k_{1a} p_{CH4} p_{O2}}{(1 + K_{CH4}^{ox} p_{CH4} + K_{O2}^{ox} p_{o2})^2} + \frac{k_{1b} p_{CH4} p_{O2}}{(1 + K_{CH4}^{ox} p_{CH4} + K_{O2}^{ox} p_{O2})} \qquad (14)$$

Steam reforming (CO production)

$$CH_4 + H_2O \Leftrightarrow CO + 3H_2 \qquad (15)$$
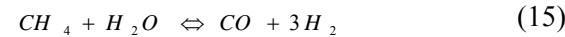
$$r_2 = \frac{k_2^{xu} / p_{H2}^{2.5} (p_{CH4} p_{H2O} - p_{H2}^3 p_{CO} / K_{eq,3})}{(1 + K_{CO} p_{CO} + K_{H2} p_{H2} + K_{CH4} p_{CH4} + K_{H2O} p_{H2O} / p_{H2})^2} \qquad (16)$$

Steam reforming (CO_2 production)

$$CH_4 + 2H_2O \Leftrightarrow CO_2 + 4H_2 \qquad (17)$$

$$r_3 = \frac{k_3^{xu} / p_{H2}^{3.5} (p_{CH4} p_{H2O}^2 - p_{H2}^4 p_{CO2} / K_{eq,4})}{(1 + K_{CO} p_{CO} + K_{H2} p_{H2} + K_{CH4} p_{CH4} + K_{H2O} p_{H2O} / p_{H2})^2} \qquad (18)$$

Water gas shift reactor mathematical model

The water gas shift reactor (WGSR) provides primary CO cleanup, as well a secondary H_2 production. In most hydrocarbon processor, the water gas shift reactor is the biggest and heaviest component because the reaction is relatively slow compared to the other reactions and is inhibited at higher temperatures by thermodynamic (Tongtaek et al., 2003). Therefore, the simulation of the WGSR reaction is based on the following set of differential equations.

Mass balance equations

$$\frac{dC_{CO}}{dt} = \left(\frac{F_{in}}{V} C_{co,in}\right) - \left(\frac{F_{out}}{V} C_{co,out}\right) - r \qquad (19)$$

$$\frac{dC_{H_2}}{dt} = \left(\frac{F_{in}}{V} C_{H_2,in}\right) - \left(\frac{F_{out}}{V} C_{H_2,out}\right) + r \qquad (20)$$

$$\frac{dC_{CO_2}}{dt} = \left(\frac{F_{in}}{V} C_{co_2,in}\right) - \left(\frac{F_{out}}{V} C_{co_2,out}\right) + r \qquad (21)$$

$$\frac{dC_{H_2O}}{dt} = \left(\frac{F_{in}}{V} C_{H_2O,in}\right) - \left(\frac{F_{out}}{V} C_{H_2O,out}\right) - r \qquad (22)$$

Energy equation

$$\frac{dT_w}{dz} = \frac{\rho_b}{u_s \rho_g C_p} \Sigma \eta_i r_i (-\Delta H_i) \qquad (23)$$

The kinetic for WGSR is known critical when designing an efficient fuel reformer and optimizing its operating conditions. So, in this paper, the reaction kinetic proposed by Yongtaek and Stenger (2003) is used as presented below. The authors derived the reaction kinetic on $Cu/ZnO/Al_2O_3$ catalyst under operating temperature between 200^oC to 250^oC.

$$CO + H_2O \Leftrightarrow CO_2 + H_2 \qquad (24)$$

$$r = k_o \exp\left(-\frac{E}{RT}\right) p_{CO}^m \, p_{H_wO}^n \, (1 - \beta) \qquad (25)$$

where

$$\beta = \frac{p_{CO_2} p_{H_2}}{p_{CO} p_{H_2O} K_{eq}}$$

Preferential oxidation reactor

The preferential oxidation reactor (PROX) is used to eliminate the CO that has not been converted in the WGSR. This reactor required to reach very low level of CO content in the fuel stream at the fuel cell inlet in order to avoid poisoning of the membrane (Zalc *et al.*, 2002). It is assumed that the PROX is operating under an isothermal condition at a temperature of 250^oC. The representative model can be described in the differential equations of mass and energy balance.

Mass balance equations

$$\frac{dC_{CO}}{dt} = \left(\frac{F_{PROXin}}{V} C_{co,in}\right) - \left(\frac{F_{PROXout}}{V} C_{co,out}\right) - r \qquad (26)$$

$$\frac{dC_{CO_2}}{dt} = \left(\frac{F_{PROXin}}{V} C_{CO2,in}\right) - \left(\frac{F_{PROXout}}{V} C_{CO2,out}\right) + r \qquad (27)$$

$$\frac{dC_{O2}}{dt} = \left(\frac{F_{PROXin}}{V} C_{O2,in}\right) - \left(\frac{F_{PROXout}}{V} C_{O2,out}\right) - 0.5r \qquad (28)$$

Energy balance equation

$$\frac{dT_{PROX}}{dt} = \left(Q_{in} + E_{rxn} - Q_{out}\right)/ Ch_{PROX} \qquad (29)$$

In this paper the kinetic of selective CO oxidation over the $Cu_{0.1}Ce_{0.9}O_{2-y}$ nanostructured catalyst can be well by employing the Liu and Flytzani-Stephanopoulus model equations (Sedmark *et al.*, 2003).

$$CO + \frac{1}{2}O_2 \Leftrightarrow CO_2 \qquad (30)$$

$$r = \frac{k_L K_L p_{CO} p_{O2}^m}{1 + K_L p_{CO}} \qquad (31)$$

where

$$k_L = A_L \exp\left(-E_{a,L}/RT\right)$$

$$K_L = B_L \exp\left(Q/RT\right)$$

Cooler Units

Two cooler units are needed in order to reduce the temperatures of the outlet gas streams from the ATR and the PROX respectively. In these equipments, the cooling water charged into the shell is from the PEM fuel cell water produce and the products of the ATR and PROX enter at the tube side. Each cooler unit have different configurations and specifications. It is assumed that the cooler unit is perfectly insulated, so that no energy lose to surrounding. Furthermore, no reaction occurs during the cooling. The models were represented by the energy balances of gases and cooling water.

First cooler unit energy balance equations
Gases

$$\frac{dT_{WGSR,in}}{dt} = \left(Q_{o,in} - Q_{o,out} - Q_{TCL1}\right)/ Ch_{CL} \qquad (32)$$

Cooling water

$$\frac{dT_{WCL}}{dt} = \left(Q_{WC,in} - Q_{WC,out} + Q_{TCL1}\right)/ Ch_{WCL} \qquad (33)$$

Second cooler unit energy balance equations
Gases

$$\frac{dT_{PEMFC,in}}{dt} = \left(Q_{o,in} - Q_{o,out} - Q_{TCL2}\right)/ Ch_{CL1} \qquad (34)$$
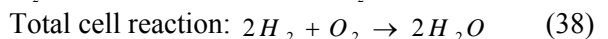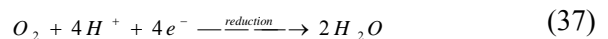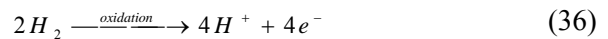
Cooling water

$$\frac{dT_{WCL}}{dt} = \left(Q_{WC,in} - Q_{WC,out} + Q_{TCL1}\right)/ Ch_{WCL} \qquad (35)$$

PEM fuel cell stack unit development

The dynamic model developed is based on appropriated energy, mass and electrochemical equations as applied to PEM fuel cell (Yerramalla *et al.*, 2003). The whole modelling process can be divided into two parts.

Individual cell modelling

The chemical reactions occurring at the oxidation and reduction electrode of a PEM fuel cell are as follows:

$$2H_2 \xrightarrow{oxidation} 4H^+ + 4e^- \qquad (36)$$

$$O_2 + 4H^+ + 4e^- \xrightarrow{reduction} 2H_2O \qquad (37)$$

Total cell reaction: $2H_2 + O_2 \rightarrow 2H_2O$ $\qquad (38)$

The various equations necessary for the modelling of an individual cell are presented below.

Butler-Volmer equation

The equation shows the net current density for one-step electrochemical reaction flowing through a metallic electrode is expressed using the following equation:

$$i = i_o \left[e^{\frac{\alpha.n.F.\eta}{R.T}} - e^{\frac{-(1-\alpha).n.F.\eta}{R.T}} \right] \qquad (39)$$

Normally the variables associated with this equation (the exchange current density i_o and the charge transfer coefficient α) are obtained from empirical procedures.

The anode overvoltage

The anode overvoltage can be represent by (Mann *et al.,* 1996):

$$\eta_{act,a} = \frac{-G_{ec}}{2F} + \frac{RT}{2F} \ln\left(4FAk_a^o c_{H2}\right) - \frac{RT}{2F} \ln i \qquad (40)$$

Equation (36) after the insertion of the known parameter values and rearrangement, gives:

$$\eta_{act,a} = -\left(5.18 \times 10^{-6}\right) \Delta G_{ec} + \left(4.309 \times 10^{-5}\right)$$
$$\times T \left[12.863 + \ln\left(\frac{Ac_{H2}k_a^o}{i}\right) \right] \qquad (41)$$

The cathode overvoltage

Again, as previously proposed ((Mann *et al.,* 1996), the cathode overvoltage can be given by

$$\eta_{act,c} = \frac{RT}{\alpha_C Fn}\left(\ln\left[nFAk\,^o_C \exp\left(\frac{-\Delta G_e}{RT}\right)\right.\right. \tag{42}$$

$$\left.\left.\times c_{O2}^{(1-\alpha c)} c_{H2}^{(1-\alpha c)} c_{H2O}^{\alpha c}\right] - \ln i\right)$$

As previously, after the insertion of the known parameter values and rearrangement, equation (38) becomes:

$$\eta_{act,c} = \frac{1}{\alpha_c}\left(-10.36\times10^{-6}\right)\Delta G_e + \left(8.62\times10^{-5}\right)$$
$$\times T\left(12.863 + \ln A + k'_c + (1-\alpha_c)\ln c_{O2}\right. \tag{43}$$
$$\left.- \ln i\right)$$

The ohmic overvoltage

The resistance to electron transfer in the graphite collector plates and graphite electrodes plus resistance to proton transfer in the solid polymer membrane produce ohmic polarization. This could be expressed using ohm's law equations such as:

$$\eta_{ohmic} = -iR^{\text{internal}} \tag{44}$$

The R^{internal} can be obtained from experimental results (Xue *et al.*, 2003)

Fuel cell stack modelling

In this section, the various equations necessary for the modelling of the overall fuel cell system are presented. For 'N' single cells connected in a fuel cell stack system, the total stack voltage (ΔVT) is calculated by:

$$\Delta V_T = NVcell \tag{45}$$

Thus, for the current of a fuel cell stack is calculated by:

$$I_{stack} = NI_{cell} \tag{46}$$

Finally the total power produced by the entire stack is calculated by multiply the total stack voltage and the current of the stack.

$$P_{stack} = \Delta V_T I_{stack} \tag{47}$$

Results and Discussion

Fuel cell system dynamic model simulation

In this section, a detailed parametric analysis to study the dynamic effects within the system was carried out. The parameters and variables used in this part of study are listed in Table 1. The model was developed under Simulink environment (Matlab 6.5.1) and as some parameters are small such as a cell volume, stiff differential equation solver ODE23S is employed in the simulation. The time length for the simulation is 3500 s.

TABLE 1 Parameters and variables used in system simulation

	Parameter	Value
D_r	Diameter of ATR, m	0.4
L_r	Length of ATR, m	0.5
T	Temperature of ATR, K,)	800
p_r	ATR operating pressure, atm	1
ρ_s	Catalyst density, kg/m^3	1870
	CH4/O2 ratio	2
	H2O/CH4 ratio	2
x_i	Species mole fraction	
C_i	Species concentration, mole/m^3	
p_i	Species partial pressure	
K_{eq}	Equilibrium Constant	
D_w	Diameter of WGSR, m	0.2
L_w	Length of WGSR, m	0.5
T_w	Initial WGSR temperature, K	523.15
P_w	WGSR operating pressure, atm	1
D_p	Diameter of PROX, m	0.1
L_p	Length of PROX, m	0.5
T_p	Initial PROX temperature, K	523.15
P_p	PROX operating pressure, atm	1
L_{WCL}	First cooler unit length, m	0.56
n	Number of tube	25
T_o	Initial cooler temperature	302.1
L_{WCL1}	Second cooler unit length, m	0.12
n	Number of tube	25
α	Transfer coefficient, anode	0.5
α	Transfer coefficient, cathode	1
F	Faraday costant, C/mole	96485
R	Universal constant of gases, J/mole.K	8.314
p_c	Air side pressure, atm	5
p_a	Fuel side pressure, atm	1
T_{cell}	Initial cell temperature, K	353.15
N	Number of cell	39
	MEA active area, cm^2	360

The parametric sensitivity of fuel cell system behaviour and its performance have been investigated for several parameters including operating temperatures and kinetic parameter. The influence of these operational parameters on the product composition depends strongly on the thermodynamics of the reactions. For this purpose, analysis has been studied over the ATR temperature of 800-1015 K and total feed flowrate from 2.0-3.0 m^3/s to see the effect on other units compositions and power production.

The results are as follow:
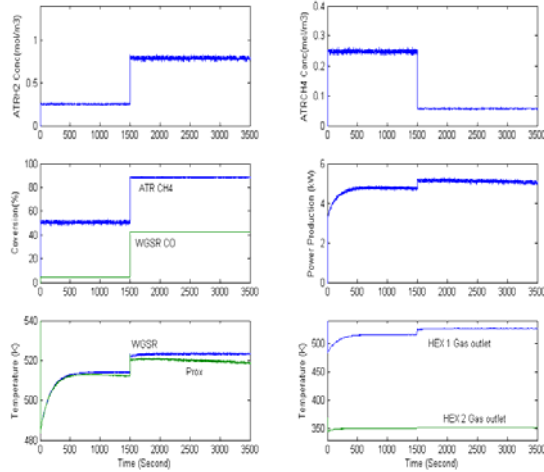1. Effect of step change in temperature

FIGURE 2   Results of step change in temperature

Figure 2 shows the CH4 and H2 concentrations of ATR, the ATR CH4 and WGSR CO conversions, the power production, the temperature of WGSR and PROX units and the gas stream temperatures of first cooler and second cooler units. While the results of step change in temperature are shown in Table 2.

TABLE 2 The Effect of step change in temperature

Parameter	800K	1015K
ATR H_2 concentration, mol/m^3	0.2469	0.7725
ATR CH_4 concentration, mol/m^3	0.2428	0.0563
ATR CH_4 conversion, %	48.86	88.15
WGSR CO conversion, %	4.242	42.81
WGSR temperature, K	514.3	523.7
PROX temperature, K	509.7	519.1
Gas stream temperature of first cooler, K	515.9	526
Gas stream temperature of second cooler, K	350.4	352
Power production, kW	4.661	5.126

From the simulation results, temperature has a significant effect on kinetic productions of hydrogen and carbon monoxide due to the increment of methane converted toward high temperature. Furthermore, the temperature of other units increase since more heat energy is supplied.

2. Effect of step change in steam feed flowrate
Figure 3 shows the ATR products concentration, the WGSR products concentration, the PROX products concentration, the conversion of CH4 for ATR and CO for WGSR and PROX. While Figure 4 indicates the power production towards step change in steam feed flowrate. The results of step change 0.5 m^3/s to 1 m^3/s in steam feed flowrate are shown in table 3.
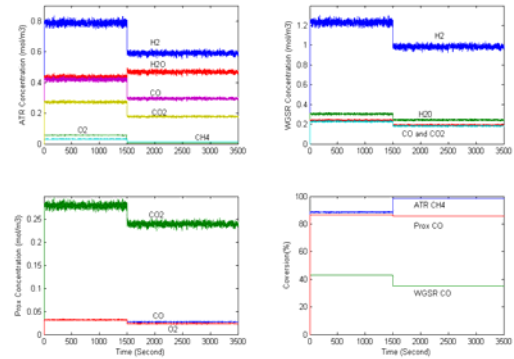

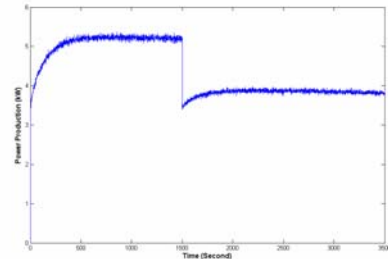FIGURE 3   Results of step change in steam feed flowrate

FIGURE 4   Power production of step change in steam feed flowrate

TABLE 3   The Effect of step change in steam feed flowrate

Parameter	0.5	1.0
ATR concentration, mol/m^3		
H_2	0.7725	0.5788
H_2O	0.4272	0.4594
CO	0.4112	0.2897
CO_2	0.2675	0.1748
O_2	0.0307	0.0148
CH_4	0.0563	0.0058
WGSR concentration, mol/m^3		
H_2	1.207	0.9657
H_2O	0.2979	0.2383
CO	0.2352	0.1881
CO_2	0.2234	0.1787
PROX concentration, mol/m^3		
CO	0.0314	0.0269
CO_2	0.2744	0.2352
O_2	0.0315	0.0230
ATR CH4 conversion, %	88.15	98.47
WGSR CO conversion, %	42.81	35.07
PROX CO conversion, %	87	85.71
Power production, kW	5.126	3.877

Base on the results, the increment of steam flowrate has a significant effect on methane consumption in ATR. Since, more steam feed to the ATR, more CH_4 is reacted. But the production of CO, CO_2 and H_2 become lower since the steam to methane ratio is constant. It is also resulted in other units' productions.

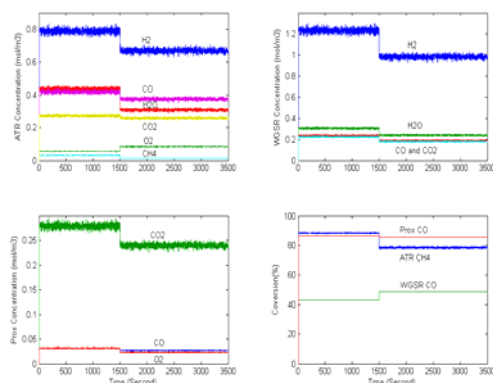3. Effect of step change in methane feed flowrate

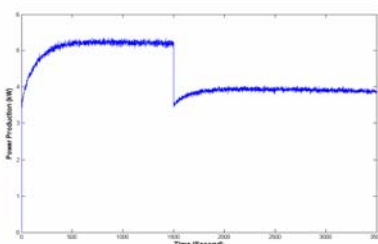FIGURE 5 Results of step change in CH_4 feed flowrate

FIGURE 6 Power production of step change in CH_4 feed flowrate

Figure 5 and figure 6 show the same parameters as figure 3 and figure 4. The results of step change 1.0 m^3/s to 2 m^3/s in methane feed flowrate are shown in Table 4.

TABLE 4 The Effect of step change in methane feed flowrate

Parameter	1.0	2.0
ATR concentration, mol/m^3		
H_2	0.7725	0.5695
H_2O	0.4272	0.2304
CO	0.4112	0.3285
CO_2	0.2675	0.2328
O_2	0.0307	0.0069
CH_4	0.0563	0.0919
WGSR concentration, mol/m^3		
H_2	1.207	0.8048
H_2O	0.2979	0.1986
CO	0.2352	0.1568
CO_2	0.2234	0.1489
PROX concentration, mol/m^3		
CO	0.0314	0.0235
CO_2	0.2744	0.2058
O_2	0.0315	0.0176
ATR CH4 conversion, %	88.15	70.95
WGSR CO conversion, %	42.81	52.28
PROX CO conversion, %	87	85
Power production, kW	5.126	3.307

In this study, the increment of methane flowrate has a significant effect on methane and oxygen consumption in ATR. Since, more methane feed to the ATR, less methane and oxygen are reacted. So, the production of CO, CO_2 and H_2 become lower since the methane to oxygen ratio is constant. It is also effected other units' productions.

From the thermodynamic analyses and kinetic simulation performed, the optimal operating conditions of the temperature is 1015 K, H_2O/CH_4 and CH_4/O_2 ratios of 2-3, feed flowrate of 2.0 m^3/s (1 m^3/s for CH_4, 0.5 m^3/s for H_2O and O_2) for ATR and fuel processor pressure at 1 atm is favourable for PEM fuel cell stack.

References
Ann De Groote, M. and Gilbert Froment, F. (1996). Simulation of the catalytic partial oxidation of methane to synthesis gas. *Applied Catalyst* 138: 245-264.

De Smet, C.R.H., De Croon, M.H.J.M., Berger, R.J., Marin, G.B. and Schouten, J.C. (2001). Design of adiabatic fixed bed reactors for the partial oxidation of methane to synthesis gas. *Application to Production of Methanol and Hydrogen-for-Fuel-Cells Science* 56:4849-4861.

Larminie, J. and Dick, A.(2000). Fuel Cell Systems, New York. Wiley.

Mann, R.F., Amphlett, J.C., Hooper, M.A.I., Jensen, H.M., Peppley, B.A. and Roberge, P.R.(2000). Development and application of a generalised steady-state electrochemical model

for a PEM fuel cell. *Journal of Power Sources* 86: 173-180.

Sedmak, G., Hocevar, S. and Levec, J. (2003). Kinetics of selective CO oxidation in excess of H2 over the nanostructured Cu0.1Ce0.9O2-y catalyst. *Journal of Catalysis* 213: 135-150.

Xu, J. and Froment, G.F. (1989). Methane Steam Reforming, Methanation and Water-gas shift: I. Intrinsic Kinitecs. *A.I.Ch.E. Journal* 35: 88-96.

Xue, X., Tang, J., Smirnova, A., England, R. and Sammes, N. (2004). System level lumped-parameter dynamic modelling of PEM fuel cell. *Journal of Power Sources* 133: 188-204.

Yerramala, S., Davari, A., Feliachi, A. and Biswas, T. (2003). Modelling and simulation of the dynamic behaviour of a polymer electrolyte membrane fuel cell. *Journal of Power Sources* 124: 104-113.

Yongtaek, C. and Stenger, H.G. (2003). Water gas shift reaction kinetics and reactor modelling for fuel cell grade hydrogen. *Journal of power Sources* 124: 432-439.

Zalc, J.M. and Loffler, D.G. (2002). Fuel processing for PEM fuel cells: transport and kinetic issues of system design. *Journal of Power Sources* 111: 58-64.